



Molecular Tagging Velocimetry in Superfluid Helium-4: Progress, Issues, and Future Development

Wei Guo¹ 

Received: 26 June 2018 / Accepted: 24 November 2018
© Springer Science+Business Media, LLC, part of Springer Nature 2018

Abstract

Helium-4 in the superfluid phase (He II) is a two-fluid system that exhibits fascinating quantum hydrodynamics with important scientific and engineering applications. However, the lack of high-precision flow measurement tools in He II has impeded the progress in understanding and utilizing its hydrodynamics. In recent years, there have been extensive efforts in developing quantitative flow visualization techniques applicable to He II. In particular, a powerful molecular tagging velocimetry (MTV) technique, based on tracking thin lines of He_2^* excimer molecules created via femtosecond laser-field ionization in helium, has been developed in our laboratory. This technique allows unambiguous measurement of the normal fluid velocity field in the two-fluid system. Nevertheless, there are two limitations to this technique: (1) only the velocity component perpendicular to the tracer line can be measured; and (2) there is an inherent error in determining the perpendicular velocity. In this paper, we discuss how these issues can be resolved by advancing the MTV technique. We also discuss two novel schemes for tagging and producing He_2^* tracers. The first method allows the creation of a tagged He_2^* tracer line without the use of an expensive femtosecond laser. The second method enables full-space velocity field measurement through tracking small clouds of He_2^* molecules created via neutron-³He absorption reactions in He II.

Keywords Quantum turbulence · Superfluid helium-4 · Flow visualization · Molecular tagging · He_2^* excimer molecules

1 Introduction

Liquid helium-4 (⁴He) transits to the superfluid phase (known as He II) below about 2.17 K [1]. In He II, two miscible fluid components coexist: an inviscid superfluid

✉ Wei Guo
wguo@magnet.fsu.edu

¹ National High Magnetic Field Laboratory, Mechanical Engineering Department, Florida State University, 1800 East Paul Dirac Drive, Tallahassee, FL 32310, USA

(i.e., the condensate) and a viscous normal fluid (i.e., the thermal excitations). The hydrodynamics of He II is strongly affected by quantum effects. For instance, the rotational motion of the superfluid component can occur only with the formation of topological defects in the form of quantized vortex lines [2]. These vortex lines all have identical cores with a radius of about 1 Å, and they each carry a single quantum of circulation $\kappa = h/m_4$, where h is Planck's constant and m_4 is the mass of a ${}^4\text{He}$ atom. Turbulence in the superfluid therefore takes the form of an irregular tangle of vortex lines (quantum turbulence) [3]. The normal fluid is expected to behave more like a classical fluid. But a force of mutual friction between the two fluids [4], arising from the scattering of thermal excitations by the vortex lines, can affect the flows in both fluids.

The fraction ratio of the two-fluid components in He II strongly depends on temperature. Above 1 K where both fluids are present, this two-fluid system exhibits fascinating hydrodynamic properties that have important scientific and engineering applications [5]. For instance, He II supports the most efficient heat transfer mechanism (i.e., thermal counterflow) and therefore has been widely utilized for cooling scientific and industrial equipment such as superconducting magnets, particle colliders, superconducting accelerator cavities, and satellites [6–8]. It has also been suggested that He II can be used to generate flows with extremely high Reynolds numbers for model testing of large-scale classical turbulence that can hardly be achieved with conventional test fluids such as water and air [9–11]. However, despite decades of research, the full potential of He II has not yet been realized, largely due to the lack of high-fidelity quantitative flow measurement tools.

Typical single-point diagnostic tools used for classical fluids, such as pitot pressure tubes and hot-wire anemometers, either have limited spatial resolution or rely on convective heat transfer that does not exist in He II. Furthermore, since the motion of both fluid components can contribute to the sensor response, data analysis can become very complicated when the two fluids have different velocity fields. More straightforward velocity measurements can be made via direct flow visualization [12]. In the past, researchers used micron-sized solidified particles as tracers and developed particle image velocimetry (PIV) and particle tracking velocimetry (PTV) techniques for He II [13–18]. These micron-sized tracers can easily get trapped on quantized vortices due to their large binding energy to the vortex cores [12]. The trapped tracers have yielded very interesting images of the vortex lines [17–20]. Nevertheless, some issues are known to exist. First, these tracer particles are produced by injecting room temperature gas mixture to liquid helium, which introduces a large heat load and hence disturbs the flow to be studied. Second, the particles produced by this method have a wide range of sizes and irregular shapes and are not neutrally buoyant, which lead to complicated tracer behavior. The strong interaction of the tracers with both the viscous normal fluid and the quantized vortices sometimes makes their motion hardly analyzable in practical turbulent flows [21]. Nevertheless, we note that in our recent PTV study of thermal counterflow in He II, a new method for separately analyzing the particles trapped on vortices and those entrained by the normal fluid approves to be very useful [22].

On the other hand, the feasibility of using He_2^* excimer molecules as tracers in He II has been validated through a series of experiments [23–25]. These molecules can

be created easily as a consequence of ionization or excitation of ground state helium atoms [27]. They have exceptionally long radiative lifetime in the electron spin triplet state (about 13 s [26]) and form tiny bubbles in liquid helium (about 6 Å in radius [27]). Due to their small size and hence small binding energy on vortex cores [28], trapping of the He_2^* tracers by quantized vortices can occur only below about 0.6 K in the absence of the normal fluid [29]. At above 1 K where most of the He II-based applications take place, He_2^* tracers are solely entrained by the normal fluid since the viscous drag force dominates other forces. These He_2^* tracers can be imaged via a cycling transition laser-induced fluorescence (LIF) technique that was developed by McKinsey's group at Yale where the author worked as a postdoctoral researcher [23,30,31]. More recently, a powerful molecular tagging velocimetry (MTV) technique based on tracking thin lines of He_2^* tracers, created via femtosecond laser-field ionization in helium, has been developed in our laboratory [32]. This technique allows for quantitative measurement of the normal fluid velocity field in the two-fluid system. The application of the MTV technique to thermal counterflow turbulence in He II has yielded remarkably fruitful results [33–38].

Nevertheless, there are two obvious limitations of this MTV technique: (1) only the velocity component perpendicular to the tracer line can be measured; and (2) there is an inherent error in determining the perpendicular velocity. In this paper, we will discuss how these issues can be resolved by creating complex tracer-line patterns for advanced MTV measurement. We will also discuss two novel schemes for tagging and producing He_2^* tracers. The first method is an inverse tagging velocimetry scheme without the use of any expensive femtosecond lasers. This method utilizes the vibrational levels of the He_2^* molecules but with much improved tagging efficiency compared to the method reported in Ref. [23]. The second method is to create small clouds of He_2^* molecules via neutron-³He absorption reactions in He II. Each small He_2^* cloud can be treated as a single “tracer” such that unambiguous PTV or PIV measurements of the normal fluid velocity field can be performed.

2 He_2^* Molecular Tagging Velocimetry: Issues and Solutions

To create a line of He_2^* tracers via laser-field ionization, laser intensity as high as 10^{13} W/cm^2 is needed [27]. This high instantaneous laser intensity can be achieved by focusing a femtosecond laser pulse in helium. In our laboratory, a regenerative amplifier laser system (wavelength λ : 780 nm, duration: 35 fs, pulse energy: up to 4 mJ) has been utilized for this purpose. As shown schematically in Fig. 1a, we focus the fs-laser beam using a lens with a focal length f and pass the beam through an optical cryostat that contains He II at regulated pressures and temperatures. Anti-reflection coated windows are used to minimize laser heating. For an ideal Gaussian beam with a beam radius ω_0 at the focal plane, one can define a Rayleigh range $Z_R = \pi\omega_0^2/\lambda$, over which the laser intensity drops by 50% due to beam spreading. The He_2^* tracers are expected to be produced essentially within the Rayleigh range. In our experiment, a fs-laser pulse energy of about 60 μJ is sufficient to create a thin line of He_2^* tracers. We then send in several pulses from a 1-kHz imaging laser at 905 nm to drive the tracers to produce fluorescent light for line imaging. Figure 1b shows a typical fluorescence

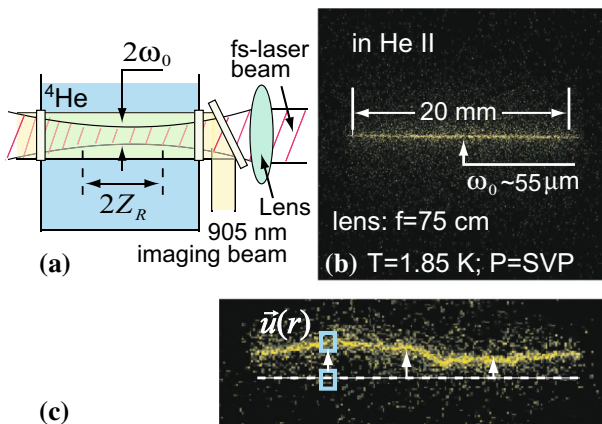


Fig. 1 **a** Schematic diagram showing the optical setup for creating and imaging He_2^* molecular tracer lines in helium. **b** A typical tracer image in He II upon its creation. **c** Schematic showing how the local velocity can be calculated. The dashed line indicates the tracer line initial location (Color figure online)

image of the He_2^* tracer line taken right after its creation in He II. The width of the tracer line is about $2\omega_0$, and its length is about $2Z_R$ as expected.

To extract velocity information, we allow an initially straight tracer line to move with the fluid by a drift time Δt . The deformed tracer line is then divided into small segments so that the center of each segment can be determined by a Gaussian fit of its intensity profile. When the drift time is small, the velocity component $u(r)$ perpendicular to the tracer line can be calculated as the vertical displacement of the line segment at r divided by Δt . Valuable flow field information, such as the streamwise velocity profile and transverse velocity correlations, can be extracted from $u(r)$. This method has been adopted in various MTV experiments in classical fluids [39,40], and it has also allowed us to obtain valuable insights in He II thermal counterflow [33–38].

Nevertheless, some limitations have been identified. First, by tracking a single tracer line, we can only determine the velocity component perpendicular to the tracer line, from which only the transverse velocity correlation at the line location can be extracted. In turbulence research, it is desirable to have the capability of mapping out the complete velocity field. Second, even for the velocity component perpendicular to the tracer lines, it is known that there is an inherent error involved in the measurement which can become nonnegligible when the flow parallel to the tracer line is sufficiently strong [41]. The first issue can be easily understood. To see the second issue more clearly, let us consider the schematic shown in Fig. 2a. An initially straight tracer line created parallel to the x -axis (i.e., the red solid horizontal line) deforms as it drifts with the fluid by a drift time Δt . If one is to measure the vertical velocity u_y at point O , our existing MTV method will yield a measured velocity $u_y^{(m)}$ that is given by $u_y^{(m)} = \Delta y_m / \Delta t$, where Δy_m is the apparent vertical displacement of point O . However, when there is a finite horizontal flow, the fluid particle originally located at point O will move to point P instead P' . Therefore, the actual vertical velocity at point O should be $u_y = \Delta y / \Delta t$. The error in the vertical velocity $\Delta u_y = u_y - u_y^{(m)}$ is thus given by

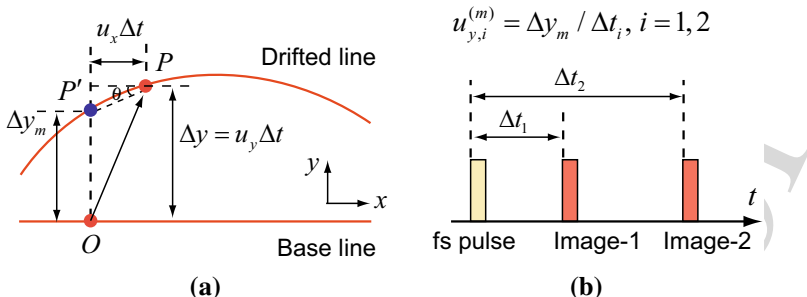


Fig. 2 **a** Schematic diagram showing the inherent error in determining the velocity component perpendicular to the tracer line. **b** Schematic diagram of the double-exposure method for correcting the inherent error (Color figure online)

$$\Delta u_y = \frac{\Delta y - \Delta y_m}{\Delta t} = \frac{u_x \Delta t \cdot \tan \theta}{\Delta t} = u_x \cdot \left(\frac{\partial u_y}{\partial x} \right) \cdot \Delta t. \quad (1)$$

One sees clearly that the error in the measured vertical velocity is proportional to both the drift time Δt and the horizontal velocity u_x . For a given drift time in an experiment, this error is negligible only if the horizontal flow is small.

To fix this issue, Hammer et al. [41] proposed a multi-time-delay approach. Here, we shall discuss a simplified double-exposure version. As illustrated in Fig. 2b, following the creation of a tracer line, we may send two imaging pulse trains at drift times of Δt_1 and Δt_2 , respectively. The camera will be synchronized with these two imaging pulse trains to capture two corresponding images of the tracer lines. For any given point O on the base line, we can now calculate two vertical velocities using the two images of the deformed line as $u_{y,1}^{(m)} = \Delta y_{m,1} / \Delta t_1$ and $u_{y,2}^{(m)} = \Delta y_{m,2} / \Delta t_2$. Note that according to Eq. 1, the actual vertical velocity u_y can be evaluated as

$$u_y = u_{y,1}^{(m)} + a \cdot \Delta t_1 \quad \text{and} \quad u_y = u_{y,2}^{(m)} + a \cdot \Delta t_2 \quad (2)$$

where the parameter $a = u_x \cdot (\partial u_y / \partial x)$. From Eq. 2, one can then determine the values for both u_y and a at the point O . Therefore, the inherent error in measuring u_y can be remedied. Note that this method assumes that the value of a does not change much between the two image acquisitions. This assumption holds when both Δt_1 and Δt_2 are small.

In principle, based on the definition of a and the obtained $u_y(x)$, one can also calculate the horizontal velocity u_x . However, this calculation involves the evaluation of spatial derivative $\partial u_y / \partial x$ from $u_y(x)$, which is normally highly noisy and undesired. A more feasible route to obtain information about other velocity components is to produce and track complex tracer-line patterns [42]. Creating multiple tracer lines simultaneously in He II is relatively straightforward using our laser system. The maximum pulse energy of our femtosecond laser (i.e., 4 mJ) is far greater than necessary for creating a single tracer line (i.e., 60 μ J [32]). Therefore, we can divide the fs-laser beam into multiple beams to produce multiple tracer lines that form patterns. Figure 3a shows the concept how the fs-laser beam can be focused into a thin laser sheet which

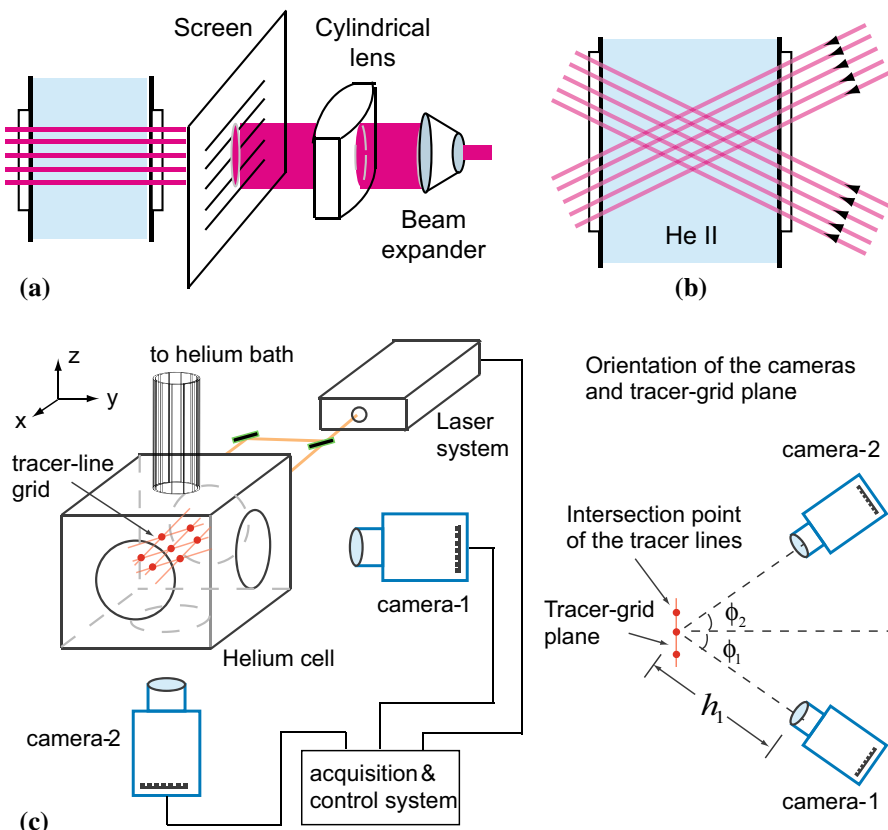


Fig. 3 Schematic diagrams of the optical systems for producing: **a** a tracer-line array and **b** a tracer-line grid. **c** Schematic diagram showing the experimental setup for stereoscopic MTV measurement in helium (Color figure online)

168 can then be passed through a screen with many parallel thin open slots for producing
 169 an array of tracer lines. Overlapping two such arrays can lead to the formation of a
 170 tracer-line grid as shown in Fig. 3b. This method has already been adopted by Hu and
 171 his colleagues in classical MTV experiments [42].

172 In order to obtain full three-dimensional (3D) velocity information, a stereoscopic
 173 imaging system needs to be implemented. Instead of tracking the tracer lines them-
 174 selves, one may track the motion of the intersection points of a tracer-line grid. These
 175 intersection points can be treated as individual “tracers” whose velocities can be accu-
 176 rately measured and are not be affected by the typical MTV inherent error. An example
 177 stereoscopic MTV setup is shown in Fig. 3c. A tracer-line grid can be created using
 178 the method as illustrated in Fig. 3b. Then, two intensified CCD (ICCD) cameras will
 179 be synchronized to take images of the tracer-line grid at the same time from two direc-
 180 tions. In a drift time dt , the apparent displacements of the intersection points of the
 181 grid-lines (i.e., those solid red dots in Fig. 3) in the imaging planes of the two cam-
 182 eras can be recorded (i.e., (dx_1, dy_1) and (dx_2, dy_2)), from which the actual x, y, z

183 displacements of the intersection points can be computed as:

$$\left. \begin{aligned} dx &= f_x(dx_1, dy_1, \phi_1, h_1, m_1; dx_2, dy_2, \phi_2, h_2, m_2) \\ dy &= f_y(dx_1, dy_1, \phi_1, h_1, m_1; dx_2, dy_2, \phi_2, h_2, m_2) \\ dz &= f_z(dx_1, dy_1, \phi_1, h_1, m_1; dx_2, dy_2, \phi_2, h_2, m_2) \end{aligned} \right\} \quad (3)$$

185 where ϕ , h , and m are the camera viewing angle, the distance between the image and
 186 the object plane, and the image magnification factor. The forms of the functions f_x , f_y ,
 187 and f_z are complex but have been discussed in great detail in the literature [43]. The
 188 three velocity components can therefore be calculated as $u_x = dx/dt$, $u_y = dy/dt$,
 189 and $u_z = dz/dt$. This velocity measurement is free from any ambiguity associated
 190 with the MTV inherent error.

191 3 Novel Schemes for Tagging and Producing He_2^* Tracers

192 3.1 Inverse Molecular Tagging Velocimetry

193 The MTV technique discussed in the previous section requires a powerful femtosecond
 194 laser system for producing He_2^* tracer lines. Such a femtosecond laser system is very
 195 expensive and normally not accessible to many research groups who would like to
 196 conduct MTV measurements in helium. On the other hand, there are many other
 197 ways to produce He_2^* molecules in helium without involving a femtosecond laser. For
 198 instance, one may use a radioactive source [31] or apply a high voltage on a sharp
 199 tungsten needle to ignite a field emission [23,25]. The He_2^* molecules produced by
 200 these methods can disperse in the whole fluid. Then, a key question is how to tag or
 201 select a group of the dispersed He_2^* molecules at a desired location for imaging so that
 202 quantitative velocity information can be obtained by tracking the tagged molecules.
 203 Ref. [23] reported a tagging method that utilizes the long-lived vibrational levels of the
 204 He_2^* triplet ground state $a^3\Sigma_u^+$. The basic concept is to use a focused nanosecond pump
 205 laser pulse at 910 nm to excite a line of He_2^* molecules from their ground state $a(0)$
 206 to the excited electronic state $c(0)$. About 4% of the $c(0)$ molecules nonradiatively
 207 decay in a few nanoseconds to the long-lived vibrational level $a(1)$ and are tagged.
 208 An expanded nanosecond probe laser at 925 nm can then be used to only drive the
 209 tagged $a(1)$ molecules to the excited d state to induce 640 nm fluorescence via the
 210 d to b transition. This method has allowed the first tagging of a He_2^* tracer line in
 211 He II thermal counterflow [25]. Nevertheless, due to the low tagging efficiency (i.e.,
 212 about 4%), many images must be superimposed at a given pump-probe delay time
 213 to achieve a good image quality. Consequently, deformations of individual lines that
 214 contain turbulent velocity field information are completed smoothed out.

215 Here we would like to discuss a new inverse tagging method that allows for high-
 216 quality imaging of individual tagged tracer lines. The scheme of this method is shown
 217 in Fig. 4a. Instead of tagging the molecules by driving them to the $a(1)$ state, a pre-
 218 pumping continuous laser at 910 nm can be used to drive the molecules from the $a(0)$ to
 219 the $c(0)$ state. Since the c to a decay time is only a few tens of nanoseconds, molecules

that decay back to $a(0)$ can quickly be re-excited to $c(0)$. Each time the molecules promoted to the $c(0)$ state have about 4% of the chance to decay to the $a(1)$ level. As a consequence, after a few excitation-decay cycles, essentially all the molecules will end up into the $a(1)$ level. A pump laser pulse at 1073 nm can now be used to excite the molecules from the $a(1)$ level to the $c(0)$ state. From the $c(0)$, about 95% of the molecules decay to the $a(0)$ state and are tagged. A probe laser pulse at 905 nm can then be used to drive only the tagged $a(0)$ molecules to the d state to produce the fluorescence. Compared to the old tagging method, this new scheme makes use of the $a(0)$ state to tag the molecules. The tagging efficiency is now 95% instead of 4%. Furthermore, for the tagged molecules in the $a(0)$ state, multiple 905 nm laser pulses can be used to drive cycling transitions to enhance the fluorescence strength. Experimentally, one may pass the fluid seeded with the $a(0)$ molecules through a region illuminated by the 910 nm pre-pumping laser so as to convert the $a(0)$ molecules into $a(1)$ s (see Fig. 4b). A focused pump laser pulse at 1073 nm tags a line of $a(0)$ molecules which is then imaged by an expanded 905 nm probe laser pulse at a delayed time. Due to the enhanced tagging and imaging efficiency, it is expected that the overall signal-to-noise ratio can be improved by two orders of magnitude compared to that in the old tagging experiment.

3.2 He_2^* Cloud Tracking Velocimetry

In classical fluid dynamics research, quantitative PIV and PTV techniques are more widely used compared to MTV measurement [44]. Unlike standard MTV where the velocity can be measured only at the locations of the tracer lines, PIV can generate a smoothly varying velocity field in the full visualization space, and PTV allows the

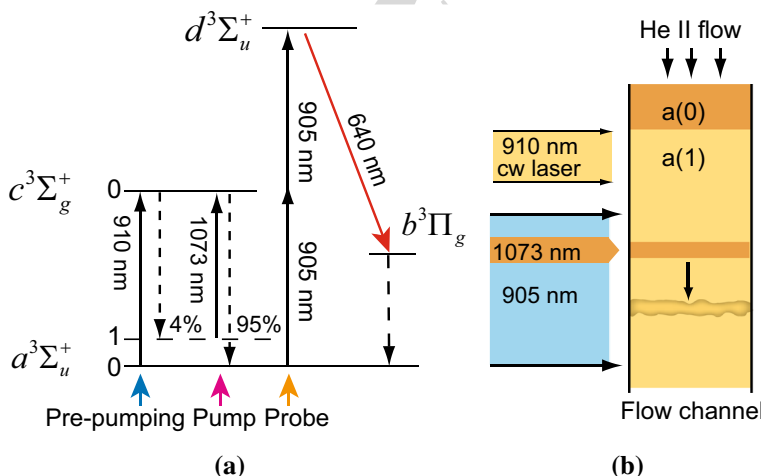
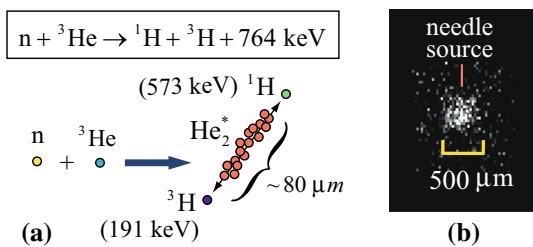


Fig. 4 **a** Schematic diagram showing the optical transitions of the inverse tagging method. The levels labeled by 0 and 1 for each electronic state are the vibrational levels of the corresponding state. **b** Schematic diagram of the experimental setup that utilizes the inverse tagging method for imaging a single tagged He_2^* tracer line (Color figure online)

Fig. 5 **a** Schematic diagram showing the neutron- ${}^3\text{He}$ absorption reaction that leads to the creation of a cloud of about 10^4He_2^* molecules. **b** A fluorescence image of a cloud of about 10^3 – 10^4He_2^* molecules, produced by applying a voltage pulse (30–60 ms) to a sharp tungsten needle in He II [23] (Color figure online)

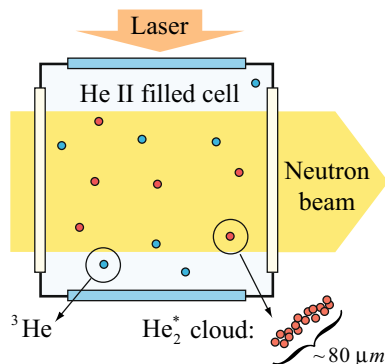


measurement of Lagrangian quantities such as the local velocity and its derivatives. In He II, PIV and PTV measurement techniques have been developed based on the use of micron-sized tracer particles [13–18]. However, the injection of these particles and their interactions with both fluid components in He II lead to known inherent issues as discussed in Sect. 1. Therefore, it is natural to ask whether it is possible to perform PIV and PTV measurements in He II with smaller tracer particles, such as He_2^* molecules. Unfortunately, the cycling transition laser-driven fluorescence scheme for detecting He_2^* molecules has not yet been pushed to the limit for imaging individual He_2^* molecules. Instead of tracking individual He_2^* molecules, a more feasible route is to develop a method to produce many small clouds of He_2^* molecules in He II and then treat each cloud as a “tracer”. Such tracer clouds can be readily imaged for traditional PIV and PTV measurements.

To create small clouds of He_2^* molecules in He II, an innovative method based on neutron- ${}^3\text{He}$ absorption reactions was first proposed by the author at a workshop on quantum turbulence held in Abu Dhabi in 2012 [45]. Then, this method was discussed in more details later at a neutron workshop at Oak Ridge National Laboratory in 2016 [46]. The basic concept is that ${}^3\text{He}$ atoms that naturally exist in He II as impurity particles can absorb neutrons as shown in the reaction schematic in Fig. 5a [47].

The absorption cross section σ depends on the energy of the incident neutrons and can be quite large for thermal neutrons that have spins aligned with the ${}^3\text{He}$ atoms (i.e., $\sigma \sim 10^{-20} \text{ cm}^2$) [48,49]. This reaction produces two charged particles, a proton (${}^1\text{H}$) and a tritium (${}^3\text{H}$), that move back to back with a total kinetic energy of 764 keV [49]. The two particles have sufficient energies to ionize and excite ground state ${}^4\text{He}$ atoms along their tracks in He II, which leads to the generation of He_2^* molecules. The total length of the two tracks, evaluated based on the known energy deposition rate of ${}^1\text{H}$ and ${}^3\text{H}$ in helium [49], is about $80 \mu\text{m}$. We can also estimate that about 10^4He_2^* molecules are produced, considering the fraction of the kinetic energy of ${}^1\text{H}$ and ${}^3\text{H}$ that goes to the generation of He_2^* molecules [50,51]. Therefore, every n - ${}^3\text{He}$ absorption event in He II creates a cloud of about 10^4He_2^* molecules with a size of about $80 \mu\text{m}$. Imaging these clouds should be feasible since we have already demonstrated high-quality fluorescence imaging of tiny clouds of He_2^* molecules created by pulsing a tungsten needle in He II (see Fig. 5b) [23]. Due to the very small molecular diffusion of He_2^* molecules in He II (i.e., $\sim 10 \mu\text{m}$ during typical drift time [30]), every cloud can be treated as a single tracer, and a spatial resolution of a few tens of microns is achievable. Tracking these He_2^* clouds should allow us to map out the full-space velocity field.

Fig. 6 Schematic of the experimental setup for producing and imaging He_2^* clouds produced via $n\text{-}^3\text{He}$ absorption reactions in He II (Color figure online)



279 Experimentally, one can pass a thermal neutron beam with a suitable flux (i.e.,
 280 $\sim 10^4/\text{cm}^2$ per pulse) through a He II filled sample cell (see Fig. 6). By adjusting
 281 the concentration of the ^3He impurity, one can conveniently tune the number density
 282 of the resulting He_2^* clouds. For instance, with a ^3He concentration as low as 50 ppm
 283 (part per million), which is far smaller than the number density of thermal rotons in
 284 He II above 1 K, we estimate that about 10^2 clouds will be produced per 1 cm^3 volume
 285 of He II, which should be sufficient for velocity field mapping purpose. This method
 286 indeed also leads to a very sensitive mechanism for neutron detection. Recently, two
 287 collaborative experimental projects have been launched on fluorescence detection of
 288 $n\text{-}^3\text{He}$ absorption events in He II. The first project was initiated by Shimizu and col-
 289 leagues at Nagoya University in collaboration with some researchers at other institutes
 290 in Japan and the author [52]. This project utilizes the neutron facilities at the Japan
 291 Proton Accelerator Research Complex (J-PARC), and its first report has been submit-
 292 ted as a proceeding paper to the 2018 International Conference on Quantum Fluids
 293 and Solids (i.e., QFS2018) [53]. The other project is being conducted at the Oak Ridge
 294 National Laboratory (ORNL) in the USA and is led by Fitzsimmons in collabora-
 295 tion with his colleagues at University of Tennessee and ORNL together with the author
 296 [54]. Preliminary results obtained in both projects have shown promising evidence for
 297 He_2^* cloud production in He II via $n\text{-}^3\text{He}$ absorption reactions.

298 4 Conclusion

299 We have briefly reviewed the progresses made in recent years in developing quantita-
 300 tive flow visualization techniques applicable to He II using He_2^* molecular tracers. A
 301 MTV technique based on tracking a thin line of He_2^* molecules created via femtosecond
 302 laser-field ionization proves to be remarkably valuable. Nevertheless, two limitations
 303 of this method have been identified. These limitations are inherent of the single-line
 304 tracking scheme. We have discussed that by creating multiple tracer lines that form
 305 a tracer-line grid, one can perform stereoscopic MTV measurements that are com-
 306 pletely immune from these limitations. Furthermore, two novel schemes for tagging
 307 He_2^* tracers are discussed. The first method involves an inverse tagging scheme that

308 greatly improves the tagging efficiency. It is expected that this method will allow the
309 tagging and imaging of a He_2^* tracer line without the use of any expensive femtosecond
310 lasers. The second method relies on the creation of small clouds of He_2^* tracers via
311 $n\text{-}^3\text{He}$ absorption reactions in He II. This method enables unambiguous quantitative
312 PTV/PIV measurements of the full-space normal fluid velocity field in He II.

313 The quantitative MTV techniques we have discussed are applicable not only to He
314 II but also to the classical phase of liquid helium (He I) and gaseous helium. They
315 have the potential to unlock the full power of cryogenic helium. For instance, helium
316 gas is particularly useful in natural thermal convection research. Heat transfer and
317 fluid flow in natural convection are controlled by the Rayleigh number Ra and the
318 Prandtl number Pr [55]. Studying the scaling laws of the flow parameters at large
319 Ra numbers, where turbulent convection sets in, is of both theoretical and practical
320 significance [56]. Close to its critical point, gaseous helium can be used to produce
321 convection flows with extremely large Ra , and the range of Ra can be tuned by a factor
322 of 10^{12} by simply adjusting the gas pressure [57–59], which makes laboratory study of
323 ocean convection and atmospheric circulation possible [56]. However, velocity field
324 measurement in helium gas has not been conducted so far, largely due to the lack of
325 appropriate tools. The development of novel He_2^* -based quantitative MTV techniques
326 may open the door for new avenues of research in this field.

327 **Acknowledgements** The author would like to acknowledge the contributions made by previous and current
328 students in the laboratory, including J. Gao, A. Marakov, E. Varga, B. Mastracci, S. Bao, Y. Zhang, and
329 H. Sanavandi. The author would also like to thank many colleagues in quantum turbulence and classical
330 fluid dynamics research fields for valuable discussions. The work has been supported by US Department
331 of Energy under Grant No. DE-FG02-96ER40952 and by the National Science Foundation under Grants
332 Nos. DMR-1807291 and CBET-1801780. All the experiments have been performed at the National High
333 Magnetic Field Laboratory, which is supported by NSF Grant No. DMR-1644779 and the state of Florida.

334 References

1. D.R. Tilley, J. Tilley, *Superfluidity and Superconductivity*, 2nd edn. (Published in association with the University of Sussex Press, Boston, 1986)
2. R.J. Donnelly, *Quantized Vortices in Helium II* (Cambridge University Press, Cambridge, 1991)
3. W.F. Vinen, J.J. Niemela, Quantum turbulence. *J. Low Temp. Phys.* **129**, 213–213 (2002)
4. W.F. Vinen, Mutual friction in a heat current in liquid helium II. I. Experiments on steady heat currents. *Proc. R. Soc. Lond. A* **240**, 114–127 (1957)
5. W. Van Sciver, *Helium Cryogenics*, 2nd edn. (Springer, New York, 2012)
6. E. Blanco, A. Calzas, J. Casas-Cubillos, P. Gomes, S. Knoops, L. Serio, R. Van Weelderen, Experimental validation and operation of the LHC Test String 2 cryogenic system. *AIP Conf. Proc.* **710**, 233–240 (2004)
7. M.A. Taber, D.O. Murry, J.R. Maddocks, K.M. Burns, Operational cryogenic experience with the gravity probe B payload. *AIP Conf. Proc.* **613**, 1241–1248 (2002)
8. A. Bonitooliva, M.B. Gorbunov, K. Iyengar, J. Miller, S.W. Van Sciver, S. Welton, Thermal-analysis of the superconducting outsert of the NHMFL 45-T hybrid magnet system. *Cryogenics* **34**, 713–716 (1994)
9. R.J. Donnelly, *High Reynolds Number Flows Using Liquid and Gaseous Helium* (Springer, New York, 1991)
10. L. Skrbek, J.J. Niemela, R.J. Donnelly, Turbulent flows at cryogenic temperatures: a new frontier. *J. Phys. Condens. Matter* **11**, 7761–7781 (1999)

354 11. K.R. Sreenivasan, R.J. Donnelly, Role of cryogenic helium in classical fluid dynamics: basic research
355 and model testing. *Adv. Appl. Mech.* **37**, 239–276 (2001)

356 12. W. Guo, D.P. Lathrop, M.L. Mantia, S.W. Van Sciver, Visualization of two-fluid flows of superfluid
357 helium-4 at finite temperatures. *Proc. Natl. Acad. Sci.* **111**, 4653 (2014)

358 13. S.W. Van Sciver, S. Fuzier, T. Xu, Particle image velocimetry studies of counterflow heat transport in
359 superfluid helium II. *J. Low Temp. Phys.* **148**, 225 (2007)

360 14. T. Zhang, S.W. Van Sciver, Large-scale turbulent flow around a cylinder in counterflow superfluid He-4
361 (HeII). *Nat. Phys.* **1**, 36 (2005)

362 15. M. La Mantia, D. Duda, M. Rotter, L. Skrbek, Lagrangian accelerations of particles in superfluid
363 turbulence. *J. Fluid Mech.* **717**, R9 (2013)

364 16. M.S. Paoletti, R.B. Fiorito, K.R. Sreenivasan, D.P. Lathrop, Visualization of superfluid helium flow. *J.*
365 *Phys. Soc. Jpn.* **77**, 111007 (2008)

366 17. G.P. Bewley, D.P. Lathrop, K.R. Sreenivasan, Superfluid helium—visualization of quantized vortices.
367 *Nature* **441**, 588 (2006)

368 18. M.S. Paoletti, M.E. Fisher, K.R. Sreenivasan, D.P. Lathrop, Velocity statistics distinguish quantum
369 turbulence from classical turbulence. *Phys. Rev. Lett.* **101**, 154501 (2008)

370 19. G.P. Bewley, M.S. Paoletti, K.R. Sreenivasan, D.P. Lathrop, Characterization of reconnecting vortices
371 in superfluid helium. *Proc. Natl. Acad. Sci.* **105**, 13707 (2008)

372 20. E. Fonda, D.P. Meichle, N.T. Ouellette, S. Hormoz, D.P. Lathrop, Direct observation of Kelvin waves
373 excited by quantized vortex reconnection. *Proc. Natl. Acad. Sci.* **111**, 4707 (2014)

374 21. D. Kivotides, Motion of a spherical solid particle in thermal counterflow turbulence. *Phys. Rev. B* **77**,
375 174508 (2008)

376 22. B. Mastracci, W. Guo, An exploration of thermal counterflow in He II using particle tracking velocime-
377 try. *Phys. Rev. Fluid* **3**, 063304 (2018)

378 23. W. Guo, J.D. Wright, S.B. Cahn, J.A. Nikkel, D.N. McKinsey, Metastable helium molecules as tracers
379 in superfluid He-4. *Phys. Rev. Lett.* **102**, 235301 (2009)

380 24. W. Guo, J.D. Wright, S.B. Cahn, J.A. Nikkel, D.N. McKinsey, Studying the normal-fluid flow in
381 helium-II using metastable helium molecules. *J. Low Temp. Phys.* **158**, 346–352 (2010)

382 25. W. Guo, S.B. Cahn, J.A. Nikkel, W.F. Vinen, D.N. McKinsey, Visualization study of counterflow in
383 superfluid 4 He using metastable helium molecules. *Phys. Rev. Lett.* **105**, 045301 (2010)

384 26. D.N. McKinsey, C.R. Brome, J.S. Butterworth, S.N. Dzhosyuk, P.R. Huffman, C.E.H. Mattoni, J.M.
385 Doyle, R. Golub, K. Habicht, Radiative decay of the metastable $\text{He}_2(a^3\Sigma_u^+)$ molecule in liquid helium.
386 *Phys. Rev. A* **59**, 200–204 (1999)

387 27. A.V. Benderskii, J. Eloranta, R. Zadoyan, V.A. Apkarian, A direct interrogation of superfluidity on
388 molecular scales. *J. Chem. Phys.* **117**, 1201–1213 (2002)

389 28. D. Mateo, J. Eloranta, G.A. Williams, Interaction of ions, atoms, and small molecules with quantized
390 vortex lines in superfluid He-4. *J. Chem. Phys.* **142**, 064510 (2015)

391 29. D.E. Zmeev, F. Pakpour, P.M. Walmsley, A.I. Golov, W. Guo, D.N. McKinsey, G.G. Ihias, P.V. McClintock,
392 S.N. Fisher, W.F. Vinen, Excimers He_2^* as tracers of quantum turbulence in 4 He in the $T = 0$
393 limit. *Phys. Rev. Lett.* **110**, 175303 (2013)

394 30. D.N. McKinsey, W.H. Lippincott, J.A. Nikkel, W.G. Rellergert, Trace detection of metastable helium
395 molecules in superfluid helium by laser-induced fluorescence. *Phys. Rev. Lett.* **95**, 111101 (2005)

396 31. W.G. Rellergert, S.B. Cahn, A. Garvan, J.C. Hanson, W.H. Lippincott, J.A. Nikkel, D.N. McKinsey,
397 Detection and imaging of He_2^* molecules in superfluid helium. *Phys. Rev. Lett.* **100**, 025301 (2008)

398 32. J. Gao, A. Marakov, W. Guo, B.T. Pawłowski, S.W. Van Sciver, G.G. Ihias, D.N. McKinsey, W.F. Vinen,
399 Producing and imaging a thin line of He_2^* molecular tracers in helium-4. *Rev. Sci. Instrum.* **86**, 093904
400 (2015)

401 33. A. Marakov, J. Gao, W. Guo, S.W. Van Sciver, G.G. Ihias, D.N. McKinsey, W.F. Vinen, Visualization
402 of the normal-fluid turbulence in counterflowing superfluid He-4. *Phys. Rev. B* **91**, 094503 (2015)

403 34. J. Gao, W. Guo, V.S. L'vov, A. Pomyalov, L. Skrbek, E. Varga, W.F. Vinen, Challenging problem in
404 quantum turbulence: decay of counterflow in superfluid 4 He. *JETP Lett.* **103**, 732 (2016)

405 35. J. Gao, W. Guo, W.F. Vinen, Determination of the effective kinematic viscosity for the decay of
406 quasiclassical turbulence in superfluid 4 He. *Phys. Rev. B* **94**, 094502 (2016)

407 36. J. Gao, E. Varga, W. Guo, W.F. Vinen, Statistical measurement of counterflow turbulence in superfluid
408 helium-4 using He_2^* tracer-line tracking technique. *J. Low Temp. Phys.* **187**, 490 (2017)

409 37. J. Gao, E. Varga, W. Guo, W.F. Vinen, Energy spectrum of thermal counterflow turbulence in superfluid
410 helium-4. *Phys. Rev. B* **96**, 094511 (2017)

411 38. J. Gao, W. Guo, W.F. Vinen, S. Yui, M. Tsubota, Dissipation in quantum turbulence in superfluid ^4He .
412 Phys. Rev. B **97**, 184518 (2018)

413 39. R.B. Miles, W. Lempert, B. Zhang, Turbulent structure measurements by relief flow tagging. Fluid
414 Dyn. Res. **8**, 9–17 (1991)

415 40. R.B. Miles, W.R. Lempert, Quantitative flow visualization in unseeded flows. Annu. Rev. Fluid Mech.
416 **29**, 285 (1997)

417 41. P. Hammer, S. Pouya, A. Naguib, M. Koochesfahani, A multi-time-delay approach for correction of
418 the inherent error in single-component molecular tagging velocimetry. Meas. Sci. Technol. **24**, 105302
419 (2013)

420 42. F. Chen, H.X. Li, H. Hu, Molecular tagging techniques and their applications to the study of complex
421 thermal flow phenomena. Acta Mech. Sin. **31**, 425 (2015)

422 43. D.G. Bohl, M.M. Koochesfahani, B.J. Olson, Development of stereoscopic molecular tagging
423 velocimetry. Exp. Fluids **30**, 302 (2001)

424 44. M. Raffel, C.E. Villert, S.T. Wereley, J. Kompenhans, *Particle Image Velocimetry—A Practical Guide*,
425 2nd edn. (Springer, Berlin, 2007)

426 45. W. Guo, New techniques for visualization study of normal-fluid turbulence in superfluid He-4 using
427 metastable He_2^* molecules. Invited talk presented at the Workshop on Turbulence in Quantum Two-
428 Fluid Systems, Abu Dhabi, UAE (05/2012)

429 46. W. Guo, Application of neutron in the study of quantum fluid hydrodynamics. Invited talk presented
430 at the Workshop on Very Cold Neutron Source for the Second Target Station Workshop, Oak Ridge
431 National Lab, Knoxville, TN, United States (05/2016)

432 47. M.E. Hayden, G. Archibald, P.D. Barnes, W.T. Buttler, D.J. Clark, M.D. Cooper, M. Espy, R. Golub,
433 G.L. Greene, S.K. Lamoreaux, C. Lei, L.J. Marek, J.C. Peng, S.I. Penttila, Neutron-detected tomog-
434 raphy of impurity-seeded superfluid helium. Phys. Rev. Lett. **93**, 105302 (2004)

435 48. L.D.P. King, L. Goldstein, The total cross section of the He-3 nucleus for slow neutrons. Phys. Rev.
436 **75**, 1366–1369 (1949)

437 49. J.S. Meyer, T. Sloan, Neutron interactions in liquid He-3. J. Low Temp. Phys. **108**, 345–354 (1997)

438 50. W. Guo, D.N. McKinsey, Concept for a dark matter detector using liquid helium-4. Phys. Rev. D **87**,
439 115011 (2013)

440 51. T.M. Ito, G.M. Seidel, Scintillation of liquid helium for low-energy nuclear recoils. Phys. Rev. C **88**,
441 025805 (2013)

442 52. Collaboration of Neutron- ^3He project at the Japan Proton Accelerator Research Complex (J-PARC):
443 T. Matsushita, V. Sonnenschein, W. Guo, H. Hayashida, K. Hiroi, K. Hirota, T. Iguchi, D. Ito, M.
444 Kitaguchi, Y. Kiyanagi, S. Kokuryu, W. Kubo, Y. Saito, H. M. Shimizu, T. Shinohara, S. Suzuki, H.
445 Tomita, Y. Tsuji, and N. Wada

446 53. T. Matsushita, V. Sonnenschein, W. Guo, H. Hayashida, K. Hiroi, K. Hirota, T. Iguchi, D. Ito, M.
447 Kitaguchi, Y. Kiyanagi, S. Kokuryu, W. Kubo, Y. Saito, H. M. Shimizu, T. Shinohara, S. Suzuki, H.
448 Tomita, Y. Tsuji, N. Wada, Generation of $^4\text{He}_2$ clusters via neutron- ^3He absorption reaction towards
449 visualization of full velocity field in quantum turbulence. J. Low Temp. Phys. (2018)

450 54. Collaboration of Neutron- ^3He project at the Oak Ridge National Lab: S. Bao, L. Crow, M. Fitzsimmons,
451 G. Greene, W. Guo, L. McDonald, T. Mezzacappa, J. Pierce, X. Tong, X. Wen, and Y. Zhao

452 55. S. Kakac, Y. Yener, A. Pramanjaroenkij, *Convective Heat Transfer*, 3rd edn. (Taylor and Francis,
453 Boca Raton, 2013)

454 56. J.J. Niemela, K.R. Sreenivasan, The use of cryogenic helium for classical turbulence: promises and
455 hurdles. J. Low Temp. Phys. **143**, 163 (2006)

456 57. J.J. Niemela, L. Skrbek, K.R. Sreenivasan, R.J. Donnelly, Turbulent convection at very high Rayleigh
457 numbers. Nature **404**, 837 (2000)

458 58. P.E. Roche, F. Gauthier, R. Kaiser, J. Salort, On the triggering of the ultimate regime of convection.
459 New J. Phys. **12**, 085014 (2010)

460 59. P. Urban, P. Hanelka, T. Kralik, V. Musilova, A. Srnka, L. Skrbek, Effect of boundary layers asymmetry
461 on heat transfer efficiency in turbulent Rayleigh–Benard convection at very high Rayleigh numbers.
462 Phys. Rev. Lett. **109**, 154301 (2012)